

Available online at [www.sciencedirect.com](http://www.sciencedirect.com)**SciVerse ScienceDirect**

Physics Procedia 36 (2012) 1002 – 1007

Physics

**Procedia**

Superconductivity Centennial Conference

# A cryogenic dc-dc power converter for a 100kW synchronous HTS generator at liquid nitrogen temperatures

Wendell Bailey<sup>a</sup> \*, Hauming Wen<sup>a</sup>, Yifeng Yang<sup>a</sup>, Andrew Forsyth<sup>b</sup>, Chungjiang Jia<sup>b</sup><sup>a</sup>*Cryogenics, Faculty of Engineering and the Environment, University of Southampton, Southampton, SO171BJ, United Kingdom*<sup>b</sup>*School of Electrical and Electronic Engineering, University of Manchester, Manchester, MN63PL, United Kingdom*

---

## Abstract

A dc-dc converter has been developed for retrofitting inside the vacuum space of the HTS rotor of a synchronous generator. The heavy copper sections of the current leads used for energising the HTS field winding were replaced by cryogenic power electronics; consisting of the converter and a rotor control unit. The converter board was designed using an H-bridge configuration with two 5A rated wires connecting the cryogenic boards to the stator control board located on the outside of the generator and drawing power from a (5A, 50V) dc power source. The robustness of converter board was well demonstrated when it was powered up from a cold start at 82K. When charging the field winding with moderate currents (30A), the heat in-leak to the 'cold' rotor core was only 2W. It continued to function down to 74K, surviving several quenches. However, the quench protection function failed when injecting 75A into the field winding, resulting in the burn out of one of the DC-link capacitors. The magnitudes of the critical currents measured with the original current leads were compared to the quench currents, which was defined as the current which triggered quench protection protocol. The difference between the two currents was rather large, (~20A). However, additional measurements using a single HTS coil in liquid nitrogen found that this reduction should not be so dramatic and in the region of 4A. Our conclusions identified the converter's switching voltage and its operating frequency as two parameters, which could have contributed to lowering the quench current. Magnetic fields and eddy currents are expected to be more prominent the field winding and its impact on the converter also need further investigation.

© 2012 Published by Elsevier B.V. Selection and/or peer-review under responsibility of the Guest Editors.

Open access under [CC BY-NC-ND license](https://creativecommons.org/licenses/by-nc-nd/4.0/).

*Keyword:* HTS generators; power converter; synchronous machines; cryogenic devices.

---

\* Corresponding author.

*E-mail address:* [wosb@soton.ac.uk](mailto:wosb@soton.ac.uk)

## 1. Introduction

Following the construction and testing of superconducting generators, which operate in the temperature range of 60K to 80K, [1-2]. A project has been carried out by a group of Universities in partnership with Rolls Royce to investigate the feasibility of building a cryogenic power converter, for energising the superconducting field winding for these types of machines. The insertion of a cryogenic dc power source onboard the cold rotor, with a high-voltage/low-current ac input and a low-voltage/high-current dc output, could reduce the heat in-leak incurred by the current leads, [3].

Cryogenic power electronics provide other promising benefits over their room temperature counterparts in terms of a reduced size, weight (increased power density), improved efficiency, improved switching speed and improved reliability. Passive devices such as inductors, capacitor and interconnects will also improve by the lowered resistance of their constituents metal conductors or use of superconductors, [4]. With the help of cryogenic power electronics; the manufacture of an HTS generator unit, fully integrated with the converter, cooling and coupling components could become a real possibility. Designers of light aircrafts, submersible sea crafts and wind farm would welcome such a generator.

## 2. Details of the HTS generator and the dc-dc power converter design

The generator selected to retro-fit the cryogenic power converter to was a 100kW synchronous generator, which used a conventional 3-phase (198A, 415V). The rotor was designed to withstand the torque generated at 3000 R.P.M and consisted of a magnetic iron core and a field winding built from a stack of ten identical HTS pancake coils, each separated by flux diverting ring. The winding had a critical current of 74.5A at 77K and had undergone an intensive test program at low temperatures, described in more detail in [5]. The calculated heat in-leak of the original current leads was 7W at 100A.

The field winding controller, shown in Figure 1(a) consisted of two parts i) the H-bridge dc-dc converter board and, ii) the control board. The function of the converter board was to charge, maintain and discharge current to the field winding. It was built using a thermally conductive PCB board and used two parallel banks of MOSFETS to help minimise conduction losses. All board components underwent cryogenic testing, to verify their suitability to operate at low temperatures. The circuit diagram in Figure 1(b) identifies the position of the converter board within the system circuit. Figures 1(c), 1(d) and 1(e) show which transistors S1, S2, S3 and S4, were active while a particular function was in operation. During the charge sequence (1a), transistors S1 and S4 were active and current was drawn from a small (5A, 50V) dc power source positioned outside the generator. The converter delivered current to the field winding in 'packets' imitating the operation of stepping power source. Once charged, S1 was opened and the current freewheeled in the closed loop (1b), formed by S2, S4 and the winding. During the discharge sequence (1c), a dump resistor was activated and the energy in the coil was dissipated through S2 and S3.

Measurement of the field winding inductance, (630 mH at low frequency and 6.8 mH at 10 kHz) and the winding resistance ( $5\Omega$  at 10 Hz and  $200\Omega$  at 10 kHz), highlighted the importance to try to minimise the operating frequency of any dc converter designed for this type of application. The maximum voltage limit for the charging circuit was set to 40V; to enable the use of cryogenically tested low-loss MOSFETS, without affecting the converters ability to charge the field winding rapidly under transient conditions. The maximum charging rate was  $\sim 2.4$ s to reach the maximum design current limit set at 150A. The control board was split into two parts; i) the rotor control board and, ii) the stator control board. The rotor control board interfaced with the dc converter and together they were fixed to the cold rotor. It was fabricated

upon a normal FR-4 PCB substrate and had three primary functions; i) control and sense the field current, ii) feedback the current signal to the stator board and execute commands sent by the stator board, iii) activate the quench protection protocol.

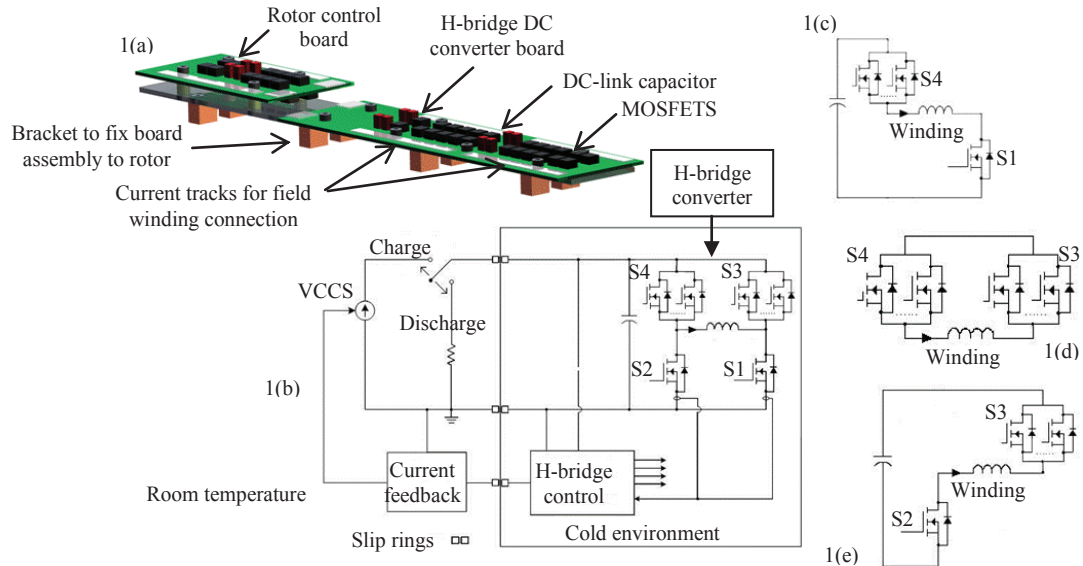


Fig.1. (a) DC converter board assembly; (b) System circuit diagram; (c) Charging circuit; (d) Freewheeling circuit; (e) Discharging circuit.

The stator control board shown in Figure 2(a), remained on the outside the machine and communicated to the ‘cold’ rotor board through a one wire link, connected via the generators 3rd slip ring. This section of the control circuit monitored the field winding current feedback signal and compared this signal to the reference current. The current feedback signal was updated at 1ms intervals. The reference current was set manually, and a PI controller generated the reference current to activate the field winding charger; a buck converter operating in peak current control mode.

### 3. Mounting of the dc-dc converter to the superconducting rotor.

The dc converter and the rotor control boards were assembled next to each other on a single aluminium support plate, which was then bolted to the side of the iron core, as shown in Figure 2(b). The final dimension of the dual board assembly was 390 mm long x 68 mm wide x 37 mm in height. The total weight of the assembly was 0.4 kg at a distance 150 mm from the centre of the machine, giving a centrifugal force of ~1500N if rotated at the balanced speed of 1500 R.P.M. In order to avoid re-balancing the rotor, only stationary tests were carried out during this project.

The heat generated by the power board when charging the field winding to ~150A, was estimated to be between 5W to 7W. Semi-flexible copper strips, soldered to the substrate of the converter board incepted the heating and compensated for the contraction of the board assembly. The other end of each strip was bolted to the ‘cold’ copper radiation shield. An HTS bus bar was soldered to each end of the field winding terminations. The other end of the bars ran parallel with the sides of the converter. Semi-flexible copper strips were used as ‘jumpers’ between the bus bar and the current tracks on the converter board.

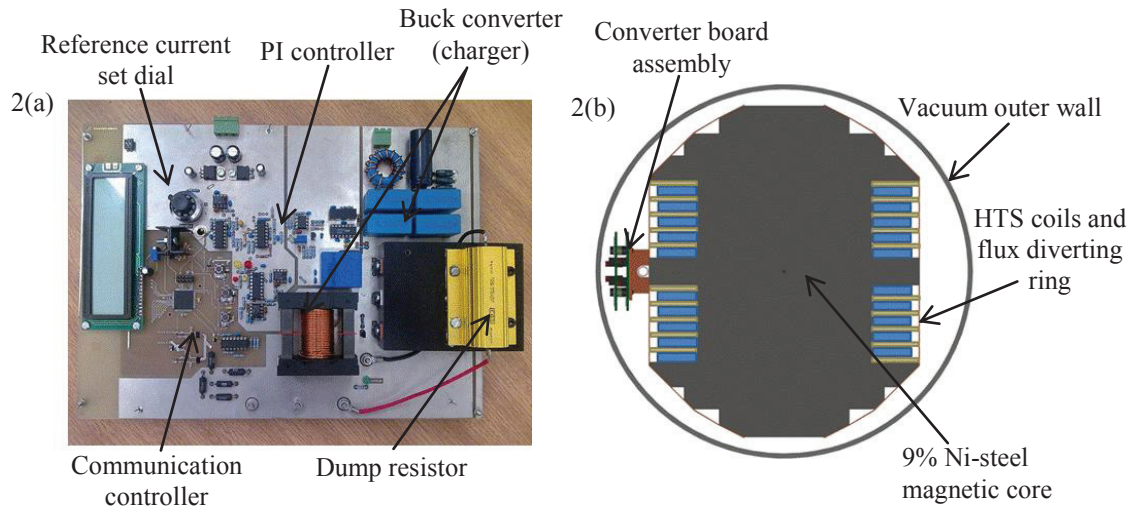


Fig.2. (a) Stator control board; (b) Cross-sectional view of the rotor assembly, the power board assembly and the vacuum outer wall.

#### 4. Testing of the dc-dc power converter

The first test for the dc converter assembly was to verify whether the board could switch on from a cold start. The rotor was cooled to 82K using liquid nitrogen delivered directly from a Dewar in an open-cycle. Figure 3(a), shows the switching waveform captured as the power electronics responded from the cold start. The square-wave (Ch 4) shows the communication signal relayed between the micro-processors onboard the rotor and stator control boards. The temperatures of the iron rotor core, a single coil in the field winding and the converter board were all monitored using wireless telemetry.

Using the closed-cycle cooling system described in [5] primed with liquid nitrogen, the rotor was cooled down to 77K. A series of board control tests were carried out up to 40A on the way down to 77K. Figure 3(b), shows a set of temperature profiles for a 40A ‘charge-freewheel-discharge cycle’. The temperature of the rotor core remained stable at ~79K throughout the cycle. The temperature of the coil reacted in conjunction with the injection of current. The temperature of the converter board also increased but lagged slightly behind that of the coil, which gave some indication about the effectiveness of the thermal links. The temperature of the coil recovered in about 5 minutes once the current was discharged.

The voltage waveforms in figure 3(c), for a 30A charge cycle were used to assess the amount of power dissipated by the converter assembly. The average power injected into the DC-link capacitor was 0.9W. The power injected through the one-wire communication line was about 1W. Therefore the additional heat load on the cryogenic cooling system due to locating the power electronics assembly in the cold environment was small (~2W at 30A). A discharge voltage waveform is presented in figure 3(c). During the transient, the current sensing power MOSFET turned on and sensed the current which was modulated and sent out by the one-wire communication system. A 47 $\Omega$  dump resistor was switched on across the ends of the DC-link capacitor. It took about 120 seconds to fully discharge the 40A freewheeling in the field winding. The trace captured the negative feedthrough current with a peak value of 0.8A

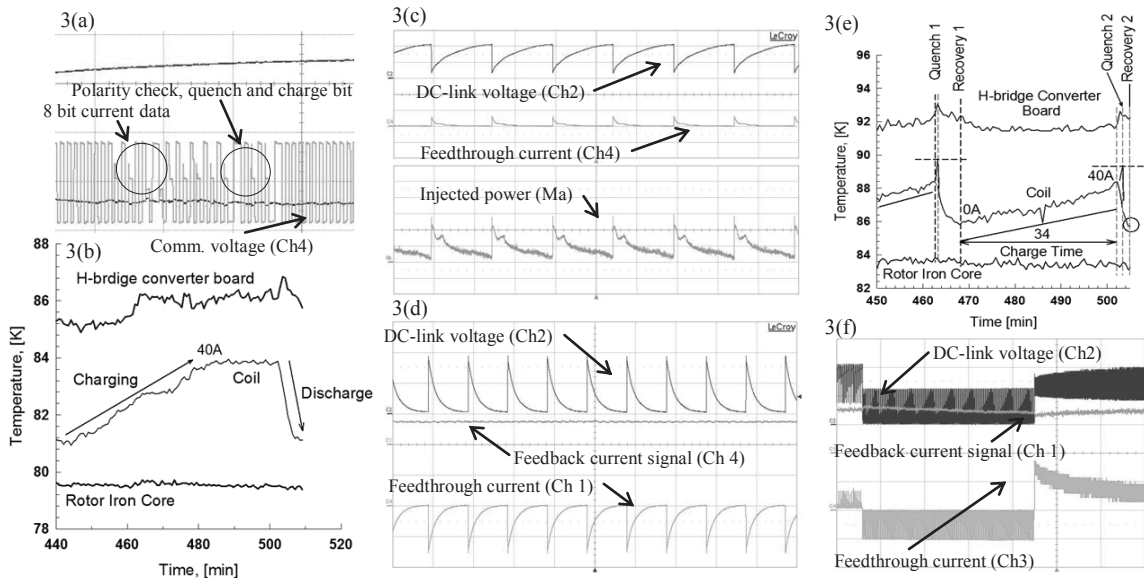


Fig.3. (a) Voltage waveform showing the operation of the one-wire communication link ( $100\mu\text{s}/\text{div}$ ), Ch4 =  $20\text{V}/\text{div}$ ; (b) Charge-freewheel-discharge cycle at  $40\text{A}$ ; (c) Voltage waveform for a  $30\text{A}$  charge cycle, ( $200\text{ms}/\text{div}$ ), Ch2 =  $20\text{V}/\text{div}$ , Ch4 =  $0.5\text{A}/\text{div}$ , Ma =  $1\text{W}/\text{div}$ ; (d) Voltage waveform for a  $40\text{A}$  discharge cycle, ( $100\text{ms}/\text{div}$ ), Ch1 =  $1\text{V}/\text{div}$ , Ch2 =  $20\text{V}/\text{div}$ , Ch4 =  $0.5\text{A}/\text{div}$ ; (e) Testing of quench protection; (f) Hysteresis control ( $5\text{s}/\text{div}$ ), Ch1 =  $0.5\text{V}/\text{div}$  equivalent to  $25\text{A}/\text{div}$ , Ch2 =  $20\text{V}/\text{div}$ , Ch3 =  $0.5\text{A}/\text{div}$

A quench protection algorithm was pre-programmed into the rotor controller. Its sensitivity was set to detect an increase in the field windings resistance of  $50\text{m}\Omega$  occurring in  $100\text{ms}$ . Within  $0.5\text{s}$ , a freewheeling pathway was opened by switching on all transistors in the H-bridge circuit to limit the onset of the quench. Figure 3(e) presents some temperature responses obtained while initiating a series of quenches in the field winding to test this function. The winding was charged to  $40\text{A}$  at  $1.2\text{A}/\text{s}$ , as the coil temperature rose from  $86\text{K}$  to  $88\text{K}$ . A current induced quench, highlighted by the sudden runaway in the coil temperature was averted as the winding protection protocol was automatically triggered. The current was safely discharged and the coil temperature fully recovered in about  $2.5$  minutes.

A second group of tests were carried out delivering liquid air from the cooling system to cool the rotor down to  $62\text{K}$  if required. The functionality of the  $5\text{A}$  hysteresis band written into the programming of the stator controller was confirmed in figure 3(f). This band prevented unnecessary switching between the charge and discharge modes during normal operation. In the waveform, the feedthrough current became negative as the circuit was switched into the discharge mode. Once the coil current decreased to  $35\text{A}$ , the circuit automatically switched back to the charge mode and the coil current began to increase to  $40\text{A}$ . Our final test was to try to inject as much current into the field winding using the dc converter system, at temperatures of  $70\text{K}$  and below. Figure 4(a) shows how the current was ramped to  $75\text{A}$  at  $5\text{A}/\text{s}$ , and the coil temperature increased to  $75\text{K}$ . Unfortunately, during an unexpected quench; the protection protocol failed and the converter board temperature suddenly increased at a much faster rate than in the coil. The result was a burn-out of one of the dc-link capacitors. Figure 4(b) presents the voltage waveform captured during this event. The feedthrough current shows a sudden spike as the energy is discharged through a weak point on the converter board and not through the dump resistor. The currents, at which the field

winding quenched when charging with the dc converter, are compared against the critical currents measured using the original copper current leads in figure 4(c). During inspection, the quench protection protocol seemed to discharge the current in the field winding prematurely; with a shortfall in current of  $\sim 20\text{A}$  seen over the entire temperature range. However, some bench-top board tests using the same quench protection criteria to protect a single HTS coil in liquid nitrogen, gave a much better agreement, (within 4A). The single coil tests were repeated several times and confirmed that the switching voltage waveform of the dc converter resulted in a slightly lower quench current. The effects of eddy currents and magnetic fields generated in the interaction between the field winding with the dc converter are unknown. Further investigation is required to see if these effects also cause reductions in the quench current.

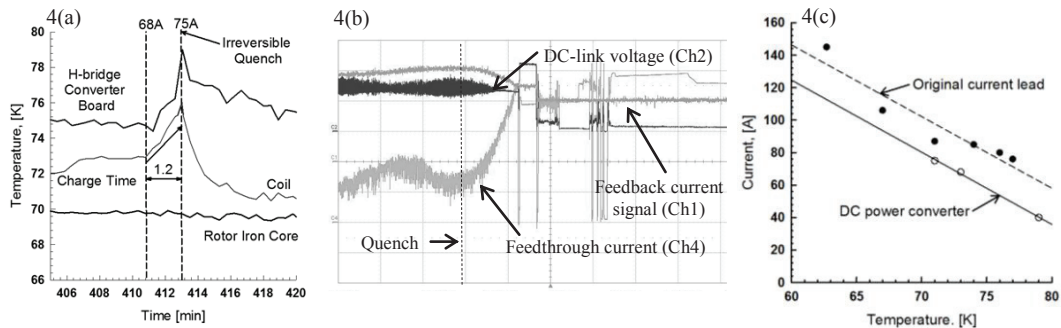


Fig.4. (a) DC converter board failure due to quench; (b) Voltage waveform during quench, Ch1= 0.5V/div equivalent to 25A/div, Ch2 = 20V/div, Ch4 = 0.5V/div; (c) Plot of the quench currents measured for the HTS winding when charging with the dc converter, compared to the critical currents obtained for the same field winding measured when using the original current leads.

## 5. Conclusions

The design of the dc-dc power converter was successful at reducing the size and weight of the power equipment needed to electrically drive an HTS generator. Potential reliability issues and heat dissipation levels were realised for such a device. The power board losses rise with the square of the winding current, although these can be further reduced by placing more MOSFETS in parallel. The current injected to the field winding before the quench protection protocol intervened was  $\sim 20\text{A}$  less than the measured critical current of the winding. Further work is needed to understand how the operating frequency and the magnitude of the switching voltage affect the quench current in order to optimise this type of power converter.

## References

- [1] Al-Mosawi MK, Goddard K, Yang Y, Beduz C. Construction of a 100 kVA high temperature superconducting synchronous generator. *IEEE Trans Appl Supercond* 2005;**15**:2182-85.
- [2] Bailey W, Goddard K, Al-Mosawi, MK, Yang, Y. The design of a lightweight HTS synchronous generator cooled by subcooled liquid nitrogen”, *IEEE Trans Appl Supercond* 2009;**19**:1674-77.
- [3] Kondo Y, Fukano S, Ninomiya A, Ishigohka T. Cryogenic low-voltage/high current dc power source using multi-parallel connected MOSFETS. *IEEE Trans Appl. Supercond* 2009;**19**:2337-40.
- [4] Haldar P et al. Improving performance of cryogenic power electronics. *IEEE Trans. Appl. Supercond* 2004;**15**:2370-75.
- [5] Wen H, Bailey W, Goddard K, Further testing of an ‘iron-cored’ HTS synchronous generator cooled by liquid air. *IEEE Trans Appl Supercond* 2011;**21**:1163-66.